


# Spin wave resonance frequency in bilayer ferromagnetic films with the biquadratic exchange interaction

Xiaojie Zhang(张晓洁), Yuting Wang(王雨汀), Yanqiu Chang(常艳秋), Huan Wang(王焕), Jianhong Rong(荣建红), and Guohong Yun(云国宏)

**Citation:**Chin. Phys. B, 2024, 33 (**9**): 097601. DOI: 10.1088/1674-1056/ad50bc
Journal homepage: http://cpb.iphy.ac.cn; http://iopscience.iop.org/cpb

**What follows is a list of articles you may be interested in**

---

## Eigenstates and temporal dynamics in cavity optomagnonics

Yun-Jing Ding(丁云静) and Yang Xiao(肖杨)
Chin. Phys. B, 2023, 32 (**10**): 107601. DOI: 10.1088/1674-1056/acf039

## Spin pumping by higher-order dipole-exchange spin-wave modes

Peng Wang(王鹏)
Chin. Phys. B, 2023, 32 (**3**): 037601. DOI: 10.1088/1674-1056/ac8922

## Theoretical investigation of ferromagnetic resonance in a ferromagnetic thin film with external stress anisotropy

Jieyu Zhou(周婕妤), Jianhong Rong(荣建红), Huan Wang(王焕), Guohong Yun(云国宏), Yanan Wang(王娅男), and Shufei Zhang(张舒飞)
Chin. Phys. B, 2022, 31 (**1**): 017601. DOI: 10.1088/1674-1056/ac1b86

## Controlled vapor growth of 2D magnetic $Cr_2Se_3$ and its magnetic proximity effect in heterostructures

Danliang Zhang(张丹亮), Chen Yi(易琛), Cuihuan Ge(葛翠环), Weining Shu(舒维宁), Bo Li(黎博), Xidong Duan(段曦东), Anlian Pan(潘安练), and Xiao Wang(王笑)
Chin. Phys. B, 2021, 30 (**9**): 097601. DOI: 10.1088/1674-1056/ac0cd9

## Effect of interface magnetization depinning on the frequency shift of ferromagnetic and spin wave resonance in YIG/GGG films

Fanqing Lin(林凡庆), Shouheng Zhang(张守珩), Guoxia Zhao(赵国霞), Hongfei Li(李洪飞), Weihua Zong(宗卫华), Shandong Li(李山东)
Chin. Phys. B, 2020, 29 (**6**): 067601. DOI: 10.1088/1674-1056/ab8dac

---

# Spin wave resonance frequency in bilayer ferromagnetic films with the biquadratic exchange interaction

Xiaojie Zhang(张晓洁)[1], Yuting Wang(王雨汀)[1], Yanqiu Chang(常艳秋)[1], Huan Wang(王焕)[2,†], Jianhong Rong(荣建红)[1,‡], and Guohong Yun(云国宏)[1,3]

[1] *Inner Mongolia Key Laboratory of Nanoscience and Nanotechnology and School of Physical Science and Technology, Inner Mongolia University, Hohhot* 010021, *China*

[2] *College of Science, Inner Mongolia Agricultural University, Hohhot* 010018, *China*

[3] *College of Physics and Electronic Information, Inner Mongolia Normal University, Hohhot* 010022, *China*

(Received 26 December 2023; revised manuscript received 27 April 2024; accepted manuscript online 28 May 2024)

The dependences of spin wave resonance (SWR) frequency on the surface anisotropy field, interface exchange coupling, symmetry, biquadratic exchange (BQE) interaction, film thickness, and the external magnetic field in bilayer ferromagnetic films are theoretically analyzed by employing the linear spin wave approximation and Green's function method. A remarkable increase of SWR frequency, except for energetically lower two modes, can be obtained in our model that takes the BQE interaction into account. Again, the effect of the external magnetic field on SWR frequency can be increased by increasing the biquadratic to interlayer exchange ratio. It has been identified that the BQE interaction is of utmost importance in improving the SWR frequency of the bilayer ferromagnetic films. In addition, for bilayer ferromagnetic films, the frequency gap between the energetically highest mode and lowest mode is found to increase by increasing the biquadratic to interlayer exchange ratio and film thickness and destroying the symmetry of the system. These results can be used to improve the understanding of magnetic properties in bilayer ferromagnetic films and thus may have prominent implications for future magnetic devices.

**Keywords:** spin wave resonance frequency, biquadratic exchange interaction, interface exchange coupling, surface anisotropy

**PACS:** 76.50.+g, 75.70.–i, 75.70.cn **DOI:** 10.1088/1674-1056/ad50bc

## 1. Introduction

Magnetic materials have been considered very attractive for various applications, including, but not limited to, communication devices[1,2] and magnetic memory devices.[3,4] Microwave oscillators with broad frequency tuning range are one of the most important components for radar and telecommunication systems, and are well known. With the rapid development of electronic communication technology, an increasing demand for higher operating frequency and higher integration density has prompted research on the application of related electronic devices in the high frequency field, especially in GHz ranges.[5,6] In this regard, the spin wave is poised to play a significant role, which can be utilized to transfer information and data with the application perspective of avoiding Joule heating and preventing energy dissipation. Moreover, in high-quality thick yttrium iron garnet films, the spin wave can carry information over distances as large as millimeters, with frequencies extending from the GHz to the THz regime, and thus offer a great opportunity for exploring the huge microwave spectrum. Many significant investigations to obtain higher resonance frequency have been accomplished in magnetic materials.[7–17] However, it is well known that the study of magnetic materials by Snoek[18] in 1947 reported that the resonance frequency of bulk magnetic materials is limited. The magnetic thin films and multilayers are expected to see further progress, with an aim towards a higher resonance frequency. Several methods have been used to study the properties of magnetic materials, such as ferromagnetic resonance (FMR), Brillouin light scattering, spin rectification effect, and spin wave resonance (SWR). Among these methods, SWR is a well-established method for intensive studies of magnetic parameters.

Spin wave theory has been investigated since the 1930s.[19] According to Holstein and Rado,[20,21] quantum spin wave theory and spin wave resonance behavior of magnetic materials were obtained. Kittel[22] first suggested that SWR might be observed in ferromagnetic thin films. Immediately, an experimental confirmation was given by Seavey and Tannenwald[23] in permalloy samples. In recent years, as reported by Qiu *et al.*,[24–31] the surface and bulk anisotropies, film thickness, interlayer coupling interaction, next-neighbor interaction, and external magnetic field are found to be beneficial for increasing SWR frequency in ferromagnetic thin films. In addition, as regards the exchange interactions, the study of high-order exchange coupling has long been a topic of great interest, including the biquadratic exchange (BQE)

†Corresponding author. E-mail: wanghuan429@163.com
‡Corresponding author. E-mail: jhrong502@163.com

© 2024 Chinese Physical Society and IOP Publishing Ltd 

interaction.[32–39] As reported by Anderson *et al.*,[40–42] the origin and magnitude of the BQE interaction can be fully explained in terms of the super-exchange mechanism. Glasbrenner *et al.*[43] confirmed that the BQE interaction is prevalent in Fe-based superconductors and cannot be neglected. On the other hand, the importance of the BQE interaction has also been demonstrated for the magnetic properties of ferromagnets[44] and antiferromagnets.[45] A previous study in a ferromagnetic thin film,[46] regarding the dependence of the SWR frequency on the BQE interaction, has obtained an enhanced SWR frequency and a widened frequency gap. However, it is not clear how the BQE interaction affects the SWR frequency in multilayer ferromagnetic films. Therefore, the present study delves into the effect of BQE interaction on the SWR frequency in bilayer ferromagnetic films using the linear spin wave approximation and Green's function method.

The rest of this paper is structured as follows. The model and Hamiltonian system are introduced in Section 2, together with the calculation procedure. In Section 3, we present the numerical solution and discuss the detailed dependence of the SWR frequency in bilayer ferromagnetic films. Finally, the paper is summarized in Section 4.

## 2. Model and calculation procedure

We assume a model of bilayer structure composed of sublayer A and sublayer B, where the sublayer A (B) consists of $N_1$ ($N_2$) monolayers located in the $y$–$z$ plane, so $N$ ($N = N_1 + N_2$) monolayers, i.e., the number of monolayers is the film thickness, are obtained (Fig. 1). There are $n$ lattices in each monolayer, so the system contains a total of $N \times n$ lattices. Here, the Hamiltonian for the present model considering a biquadratic term is given by

$$\begin{aligned} H = & -\sum_{l,l'=1}^{N_1}\sum_{i,i'} J_{1\mathrm{A}} S_{li} S_{l'i'} - \sum_{l,l'=N_1+1}^{N}\sum_{i,i'} J_{1\mathrm{B}} S_{li} S_{l'i'} \\ & - \sum_{l,l'=N_1,N_1+1}\sum_{i,i'} J_{\mathrm{AB}} S_{li} S_{l'i'} \\ & - \sum_{l,l'=1}^{N_1}\sum_{i,i'} J_{2\mathrm{A}} (S_{li} S_{l'i'})^2 - \sum_{l,l'=N_1+1}^{N}\sum_{i,i'} J_{2\mathrm{B}} (S_{li} S_{l'i'})^2 \\ & - \sum_{(l=1,N)i} g\mu_0 K_{\mathrm{Sl}} S_{li}^z - \sum_{li} g\mu_{\mathrm{B}} B_0 S_{li}^z, \end{aligned} \tag{1}$$

where $S_{li}$ ($S_{l'i'}$) represents the spin operators acting on magnetic sites $i$ ($i'$) on the monolayers $l$ ($l'$). $J_{1\mathrm{A}}$ ($J_{1\mathrm{B}}$) and $J_{2\mathrm{A}}$ ($J_{2\mathrm{B}}$) stand for the interlayer and biquadratic exchange constants, respectively, and the summations in the first two terms are taken over all pairs of nearest neighbor sites. $J_{\mathrm{AB}}$ denotes the interface exchange coupling between sublayer A and sublayer B. Parameter $\alpha_i$ ($i = \mathrm{A}, \mathrm{B}$) is defined in terms of the ratio of the biquadratic to interlayer exchange ($\alpha_{\mathrm{A}} = J_{2\mathrm{A}}/J_{1\mathrm{A}}$, $\alpha_{\mathrm{B}} = J_{2\mathrm{B}}/J_{1\mathrm{B}}$).[44,45] We have also considered the Zeeman energy with the external magnetic field along the $z$-axis and the surface anisotropy energy of the up and down film, where $g$ is the Landé factor, $K_{\mathrm{S}}$ is the surface anisotropy field and $B_0$ is an external magnetic field. $\mu_0$ and $\mu_{\mathrm{B}}$ represent the vacuum magnetic permeability and the Bohr magneton, respectively. Using the Holstein–Primakoff transform ($a^+$ and $a$ are creation and annihilation operators, respectively)

$$\begin{aligned} S^+ &= \sqrt{(2s - a^+ a)}\, a, \\ S^- &= a^+ \sqrt{(2s - a^+ a)}, \\ S^z &= s - a^+ a, \end{aligned} \tag{2}$$

the linear spin wave approximation, and introducing the spin wave operators $b_{lk_\parallel}$ ($b_{lk_\parallel}^+$) ($l = 1 \sim N$). Here, our model considers homogeneous ferromagnetic bilayer materials, setting $J_{1\mathrm{A}} = J_{1\mathrm{B}} = J_1$, $J_{2\mathrm{A}} = J_{2\mathrm{B}} = J_2$, $\alpha_{\mathrm{A}} = \alpha_{\mathrm{B}} = \alpha$ and $K_{\mathrm{SA}} = K_{\mathrm{SB}} = K_{\mathrm{S}}$. So, Eq. (1) can be rewritten as

$$\begin{aligned} H = & -6nS^2 J_1 \left(N - \frac{2}{3}\right) - 2nS^2 J_{\mathrm{AB}} - 6nS^2 J_2 \left(N - \frac{2}{3}\right) \\ & - \sum_{l=1,N} g\mu_0 K_{\mathrm{S}} nS - Nng\mu_{\mathrm{B}} B_0 S \\ & + \sum_{l=2(l\neq N_1,N_1+1)}^{N-1} (12J_1 S + 24J_2 S^3 + g\mu_{\mathrm{B}} B_0) \sum_{k_\parallel} b_{l,k_\parallel}^+ b_{l,k_\parallel} \\ & + \sum_{l=1,N} (10J_1 S + 20J_2 S^3 + g\mu_{\mathrm{B}} B_0 + g\mu_0 K_{\mathrm{S}}) \sum_{k_\parallel} b_{l,k_\parallel}^+ b_{l,k_\parallel} \\ & + \sum_{l=N_1,N_1+1} (10J_1 S + 2J_{\mathrm{AB}} S + 20J_2 S^3 + g\mu_{\mathrm{B}} B_0) \sum_{k_\parallel} b_{l,k_\parallel}^+ b_{l,k_\parallel} \\ & - \sum_{l=1}^{N} (4J_1 S + 8J_2 S^3) \sum_{k_\parallel} \gamma_{k_\parallel} (2 b_{l,k_\parallel} b_{l,k_\parallel}^+ - 1) \\ & - \sum_{l=1(l\neq N_1)}^{N-1} (2J_1 S + 4J_2 S^3) \sum_{k_\parallel} (b_{l,k_\parallel} b_{l+1,k_\parallel}^+ + b_{l,k_\parallel}^+ b_{l+1,k_\parallel}) \\ & - \sum_{l=N_1}^{N_1+1} 2J_{\mathrm{AB}} S \sum_{k_\parallel} (b_{l,k_\parallel} b_{l+1,k_\parallel}^+ + b_{l,k_\parallel}^+ b_{l+1,k_\parallel}). \end{aligned} \tag{3}$$

Note that

$$\gamma_{k_\parallel} = \frac{1}{4} \sum_{\delta_\parallel} \mathrm{e}^{\mathrm{i} k_\parallel \delta_\parallel}, \tag{4}$$

where $\delta_\parallel$ denotes only the exchange interactions between the nearest neighbor lattices in the $y$–$z$ plane, so that $\gamma_{k_\parallel}$ is real according to the lattice symmetry.

We define the $N$-order matrix retarded Green's function as follows:

$$G(k_\parallel, f) = [G_{i,j}]_{N\times N}. \tag{5}$$

Here,

$$G_{i,j} = \left\langle \left\langle b_{ik_\parallel}; b_{jk_\parallel}^+ \right\rangle \right\rangle_f, \quad (i = 1 \sim N;\ j = 1 \sim N). \tag{6}$$

The solution of the Green's function is as follows:

$$G(k_\parallel, f) = \frac{1}{\det(D(f))} [M_{i,j}]_{N\times N}, \tag{7}$$

where the matrix $M$ is the adjoint matrix of the matrix $D(f)$, and

$$D(f) = [W_{ij}]_{N\times N} + [H_{ij}]_{N\times N}. \tag{8}$$

For the $N$-order $W$ matrix, the diagonal element is $f$ representing the resonance frequency of the system and all other matrix elements are zero. The matrix elements $H_{ij}$ $(i, j = 1 \sim N)$ of the three-diagonal matrix $H$ are as follows:

$$\begin{aligned}
H_{i,i} &= 8J_1S(1-\gamma_{k_\parallel}) + 4J_1S + 24J_2S^3 \\
&\quad - 16J_2S^3\gamma_{k_\parallel} + g\mu_B B_0, \\
&\quad (i = 2 \sim (N-1),\ i \neq N_1, N_1+1), \\
H_{1,1} &= H_{N,N} = 8J_1S(1-\gamma_{k_\parallel}) + 2J_1S + 20J_2S^3 \\
&\quad - 16J_2S^3\gamma_{k_\parallel} + g\mu_B B_0 + g\mu_0 K_S, \\
H_{N_1,N_1} &= H_{N_1+1,N_1+1} = 8J_1S(1-\gamma_{k_\parallel}) + 2J_1S + 2J_{AB}S \\
&\quad + 20J_2S^3 - 16J_2S^3\gamma_{k_\parallel} + g\mu_B B_0, \\
H_{i,i+1} &= 2J_1S + 4J_2S^3, \quad (i = 1 \sim (N-1),\ i \neq N_1), \\
H_{i,i-1} &= 2J_1S + 4J_2S^3, \quad (i = 2 \sim N,\ i \neq N_1+1), \\
H_{N_1,N_1+1} &= H_{N_1+1,N_1} = 2J_{AB}S.
\end{aligned} \tag{9}$$

The $N$ numerical solutions of the SWR frequency of the bilayer ferromagnetic films and the dependence of the SWR frequency on the BQE interaction occurring on the nearest neighbor sites were obtained by solving $\det(D(f)) = 0$.

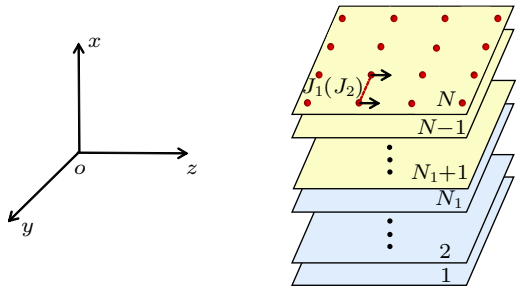



**Fig. 1.** A sketch of the present model for bilayer ferromagnetic films. Red and black dots indicate lattice sites and layers, respectively.

Here, it should be pointed out that the model is described without considering the presence of dipole–dipole interaction, because of $k_\parallel = 0$.[47,48] For convenience, we show the numerical calculations in units of the spin quantum number $S$.

## 3. Results and discussion

The biquadratic to interlayer exchange ratio $\alpha$ dependence of SWR frequency is demonstrated in Fig. 2 for symmetric $(N_1 = N_2)$ and asymmetric systems $(N_1 \neq N_2)$. For the numerical calculations, the following parameters are considered: spin quantum number $S = 1$, surface anisotropy field $K_S = 1$, interlayer exchange coupling $J_1 = 1$, interface exchange coupling $J_{AB} = 0.5$, and external magnetic field $B_0 = 0$, respectively. Considering that the two ferromagnetic thin film consists of $N = 12$ monolayers, 12 SWR modes are obtained, where $m = 1, 2, \ldots, N$ indicating the mode number of spin wave modes starting from the energetically lowest mode. It can be seen from Fig. 2(a) that a linear increase of the SWR frequency occurs by increasing the biquadratic to interlayer exchange ratio $\alpha$. Note that the value for $\alpha$ does significantly affect the energetically mid-higher modes, but does insignificantly affect the energetically lower two modes. This shows that the effect of the BQE interaction on the energetically lowest mode which is a uniform mode is weaker. At the same time, the frequency gap between the energetically highest mode and lowest mode can also be considerably increased by increasing the biquadratic to interlayer exchange ratio $\alpha$. However, as the mode number increases, the frequency gap between neighbor modes is initially narrow and then varies repeatedly between wider and narrower in symmetric bilayer ferromagnetic films. The frequency gap between the energetically higher two modes appears narrower compared to the other gaps between neighbor modes. These results suggest that the presence of the BQE interaction is rather important for achieving a larger SWR frequency and a wider frequency gap between the energetically highest mode and lowest mode.

Moreover, a visible change in the biquadratic to interlayer exchange ratio $\alpha$ dependence of the SWR frequency $(m \neq 1, 2)$ is obtained as the symmetry of the system is destroyed [see Figs. 2(b) and 2(c)]. In asymmetric bilayer films, there is an irregular variation of the frequency gap between the neighbor modes as the mode number increases, which is different from the variation of the frequency gap shown in symmetric bilayer ferromagnetic films. In order to understand the effect of symmetry more clearly, the slope is calculated by taking the derivative of the SWR frequency with respect to the biquadratic to interlayer exchange ratio $\alpha$. The slopes $(\mathrm{d}f/\mathrm{d}\alpha)$ of each mode for symmetric and asymmetric systems as a function of mode numbers are presented in Fig. 2(d). With the continuous destruction of the symmetry of the system, except for the middle modes $m = 6, 7, 8, 9$, the SWR frequency of the other even modes (odd modes) is monotonously changed. For the even modes $(m = 4, 10, 12)$, SWR frequency increases as the symmetry of the system is destroyed; while the opposite occurs at the odd modes $(m = 3, 5, 11)$, where SWR frequency is decreased. On the other hand, as the symmetry of the system is continuously destroyed, the spectrum curves for $m = 6$, 8 $(m = 7, 9)$ shift first towards higher (lower) values and then towards the lower (higher) values. The slope clearly reflects the different sensitivities of different modes to the symmetric and asymmetric systems.

In order to see how the film thickness impacts the SWR frequency in the bilayer ferromagnetic films, the SWR frequency versus the biquadratic to interlayer exchange ratio $\alpha$ for different thicknesses of the symmetric bilayer films are

plotted as shown in Fig. 3. Other parameters here for the bilayer films were kept the same as Fig. 2. As can be seen in Fig. 3, the increase of the film thickness results in a lower SWR frequency of modes $m \leq 8$. Contrary to that obtained for the variations of the SWR frequency of the energetically mid-lower modes, the energetically highest mode in thicker film is higher than those in thinner film. On the other hand, upon increasing film thickness, the curves of neighbor modes move in closer proximity to each other. Namely, the frequency gap between neighbor modes decreases with the increase of the film thickness. This means that the effect of thickness becomes weaker for energetically higher modes when the film is thicker.

To achieve a deeper comprehension of the SWR frequency, we analyze in detail the effect of the different symmetric and asymmetric systems and film thicknesses on the SWR frequency of the energetically lower four modes and the frequency gap between the energetically highest mode and lowest mode, as displayed in Fig. 4. Here, the different symmetric and asymmetric systems and film thicknesses are represented by solid, dashed, and dotted lines, respectively, and different colored lines represent different modes (black $m = 1$; red $m = 2$; blue $m = 3$; green $m = 4$). The SWR frequency of the energetically lower four modes linearly increases by increasing the biquadratic to interlayer exchange ratio $\alpha$ [see Fig. 4(a)]. There occurs a decrease (increase) of the SWR frequency for mode $m = 3$ ($m = 2$, 4) as the symmetry of the system is destroyed. However, the SWR frequency of the energetically lowest mode is found to be almost unaffected by the symmetry. In addition, as illustrated in Fig. 4(b), increasing film thickness leads to a decrease of the SWR frequency of the energetically lower four modes and a narrower frequency gap between neighbor modes occurs. This is probably because the interface exchange interaction of the thicker film is weaker than the thinner one.

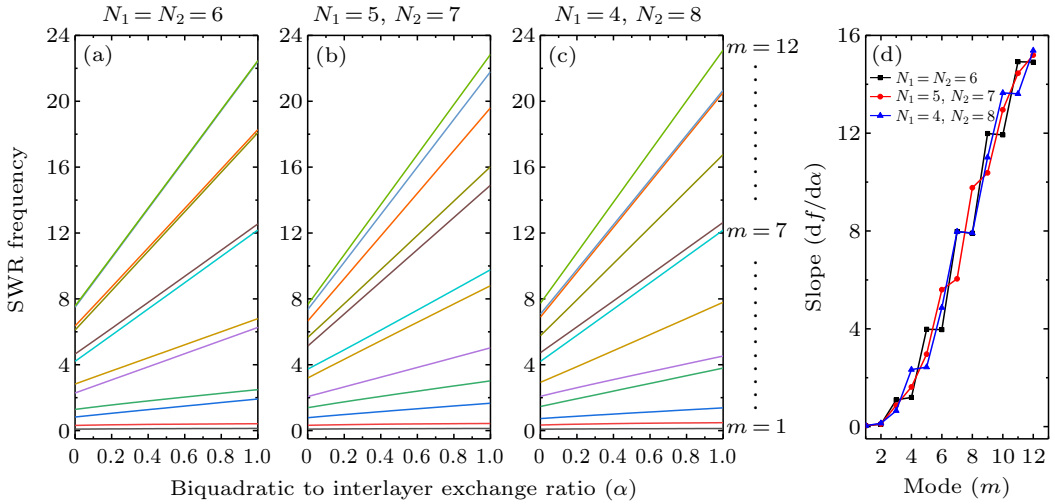



**Fig. 2.** SWR frequency as a function of the biquadratic to interlayer exchange ratio $\alpha$ for symmetric and asymmetric systems with $S = 1$, $J_{AB} = 0.5$, $K_S = 1$ and $B_0 = 0$. (a) $N_1 = N_2 = 6$, (b) $N_1 = 5$, $N_2 = 7$, and (c) $N_1 = 4$, $N_2 = 8$. (d) Slope (the derivative of SWR frequency with respect to the biquadratic to interlayer exchange ratio $\alpha$) as a function of the different modes for symmetric and asymmetric systems.

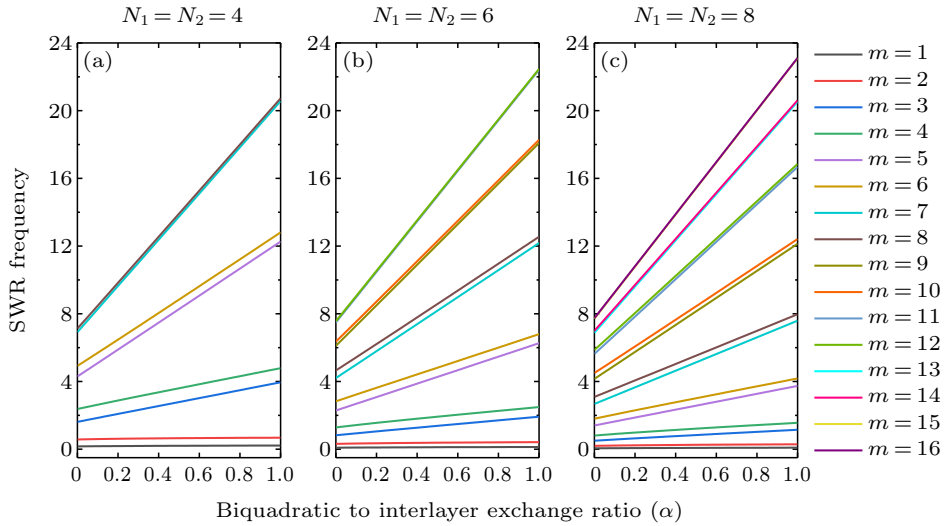



**Fig. 3.** SWR frequency as a function of the biquadratic to interlayer exchange ratio $\alpha$ for different film thicknesses. (a) $N = 8$, (b) $N = 12$, and (c) $N = 16$. Other parameters are chosen to be the same as before.

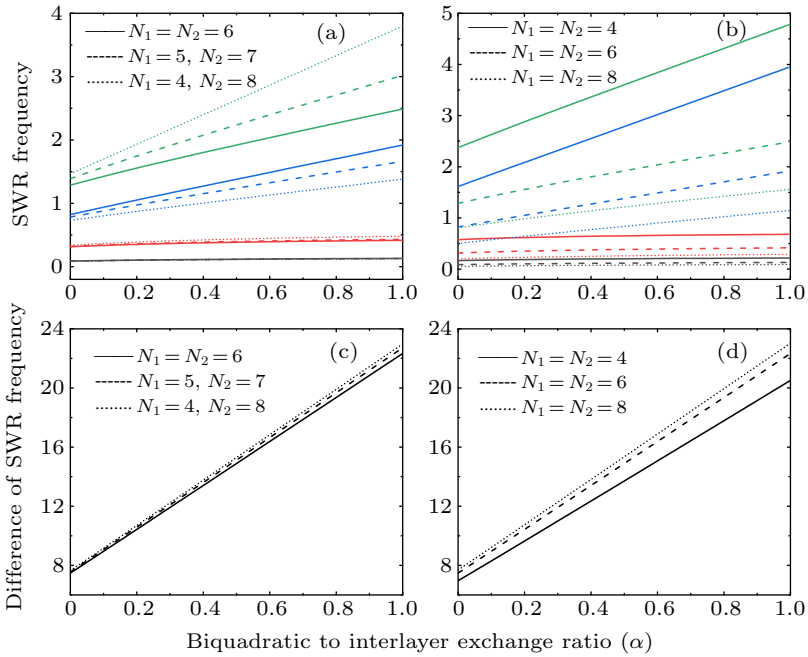



**Fig. 4.** Biquadratic to interlayer exchange ratio $\alpha$ dependence of the SWR frequency of the energetically lower four modes for different (a) symmetric and asymmetric systems and (b) film thicknesses. Different colored lines represent different modes, respectively. Biquadratic to interlayer exchange ratio $\alpha$ dependence of the SWR frequency difference between the energetically highest and lowest modes for different (c) symmetric and asymmetric systems and (d) film thicknesses.

On the other hand, the frequency gap between the energetically highest mode and lowest mode increases by increasing the biquadratic to interlayer exchange ratio $\alpha$ and destroying the symmetry [see Fig. 4(c)], while the symmetry has a rather small effect on the frequency gap. The increase of the film thickness is also accompanied by an increase of the frequency gap between the energetically highest and lowest modes obtained in bilayer films [see Fig. 4(d)]. In contrast, the film thickness dependence of the frequency gap appears larger than the symmetry dependence. Based on these dependencies, it can be concluded that film thickness and symmetry are very important for improving the SWR frequency.

The variations of the SWR frequency of the energetically lower and higher three modes with the surface anisotropy field are given in Fig. 5 for different symmetric and asymmetric systems and film thicknesses. Here, the solid, dashed, dashed–dotted, and dotted lines represent the spectrum curves of the different systems $N_1 = 4$, $N_2 = 8$; $N_1 = 5$, $N_2 = 7$; $N_1 = N_2 = 6$ and $N_1 = N_2 = 8$, respectively, and different colored lines represent different modes. For the energetically lower three modes, there is a pronounced increase of the SWR frequency by increasing the surface anisotropy field [see Fig. 5(a)]. Moreover, for the energetically lowest mode ($m = 1$), it is shown that the overlap of the spectrum curves for the symmetric and asymmetric systems at fixed film thickness and that the surface anisotropy field dependence of the SWR frequency decreases with increasing film thickness. This agrees with the results reported in Ref. [26]. In asymmetric bilayer films, the effect of the surface anisotropy field on the SWR frequency of even (odd) mode $m = 2$ ($m = 3$) is much larger (lower) than in symmetric bilayer films. For the energetically higher three modes, the curves of the SWR frequency in Fig. 5(b) exhibit little variation as the surface anisotropy field increases. In particular, the SWR frequency of the energetically highest mode is almost independent of the surface anisotropy field for the bilayer films. In addition, for the symmetric bilayer films, the SWR frequency of the energetically highest mode increases as the film thickness is increased. It is also found that the SWR frequency of the energetically highest mode at the same film thickness increases as symmetry is destroyed. On the other hand, the frequency gap between the energetically higher two modes is increased by reducing the film thickness and destroying the symmetry of the bilayer films.

To examine the dependence of the SWR frequency on the external magnetic field in our system, the spectrum curves of all modes are plotted as a function of the external magnetic field in Fig. 6 with $S = 1$, $J_{AB} = 0.5$ and $K_S = 1$. Here, the solid and dashed lines represent the spectrum curves of the symmetric system ($N_1 = N_2 = 6$) and asymmetric system ($N_1 = 4$, $N_2 = 8$), respectively. One can see that a larger SWR frequency has been obtained in the stronger external magnetic field, while the frequency gap between the neighbor modes does not depend on the external magnetic field [see Fig. 6(a)]. Even more significant enhancement of SWR frequency was attained after the biquadratic to interlayer exchange ratio $\alpha$ increased, whereas the energetically lower two modes are less affected by the value for $\alpha$ [see Figs. 6(b) and 6(c)]. In addition, for the even modes ($m = 4$, 6, 8, 10, and 12), the SWR frequency in the bilayer films shifts towards the higher val-

ues by destroying symmetry, which is opposite to the behavior shown at the odd modes ($m = 3$, 5, 9, and 11). However, the spectrum curves of mode $m = 7$ for the symmetric system and asymmetric system are indistinguishable.

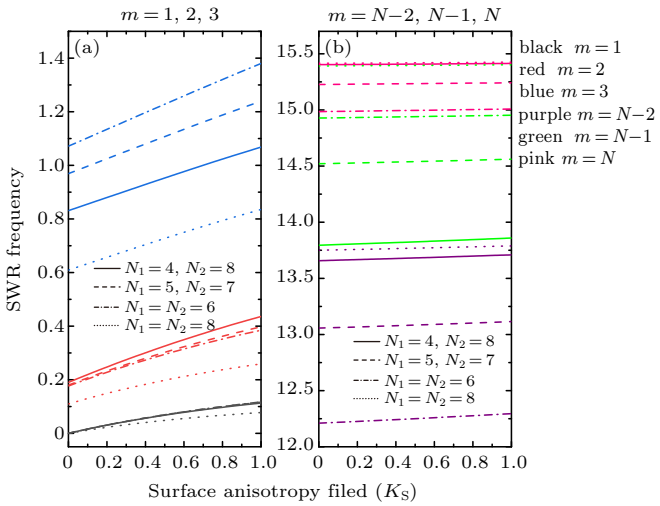



**Fig. 5.** SWR frequency as a function of the surface anisotropy field for the (a) energetically lower three modes and (b) energetically higher three modes with different symmetric and asymmetric systems and film thicknesses. Other calculated parameters are $S = 1$, $J_{AB} = 0.5$, $B_0 = 0$ and $\alpha = 0.5$.

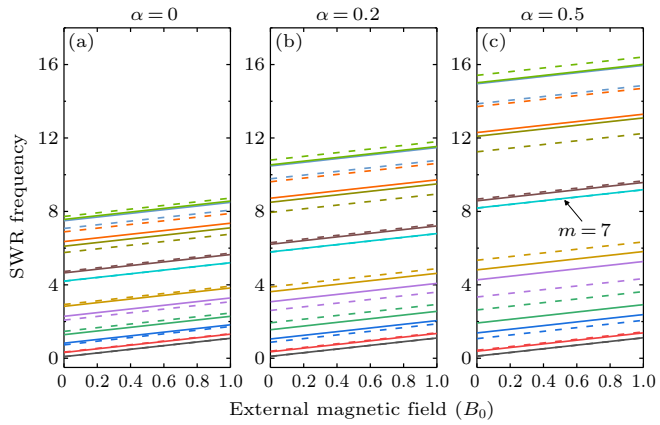



**Fig. 6.** External magnetic field dependence of the SWR frequency for different biquadratic to interlayer exchange ratios $\alpha$ with $S = 1$, $J_{AB} = 0.5$ and $K_S = 1$, for the symmetric system (solid lines) and asymmetric system (dashed lines), respectively. (a) $\alpha = 0$, (b) $\alpha = 0.2$, and (c) $\alpha = 0.5$.

In order to get a clear understanding of the effect of the interface exchange coupling, we investigated the variation of the SWR frequency as a function of the interface exchange coupling for symmetric and asymmetric systems, as depicted in Fig. 7. The different colored lines represent different modes, as in Fig. 3. For the symmetric bilayer ferromagnetic films ($N_1 = N_2 = 6$), the SWR frequency of the odd modes exhibited no dependence on the interface exchange coupling, whereas an increase of the even modes is obtained by increasing interface exchange coupling [see Fig. 7(a)]. This is consistent with the results reported in Ref. [25]. The variations of the SWR frequency of the middle modes $m = 4$, 6, 8 are more pronounced than those of the other modes. It follows that in symmetric bilayer ferromagnetic films, the main effects of the interface exchange coupling occur for the SWR frequency of even modes. Accordingly, it is noted that there is a significant increase of the frequency gap between the modes $m = n$ ($n = 1$, 3, 5, 7, 9, 11) and $m = n+1$ as interface exchange coupling increases. At the same time, the frequency gap first increases as mode number ($m \leq 6$) increases and then gradually decreases for higher modes ($m > 6$). For the asymmetric bilayer ferromagnetic films ($N_1 = 4$, $N_2 = 8$), the SWR spectrum curves of modes $m = 1$, 4, 7, 10, 12 are almost parallel to the horizontal axis [see Fig. 7(b)]. However, for the other modes, interface exchange coupling leads to an increase of the SWR frequency, especially for modes $m = 5$, 8. Moreover, the frequency gap between the energetically highest mode and lowest mode is slightly increased with the increase of the interface exchange coupling for the symmetric ferromagnetic films [see Fig. 7(c)]. However, it can be seen that for the asymmetric ferromagnetic films, the frequency gap does not monotonously change by increasing interface exchange coupling.

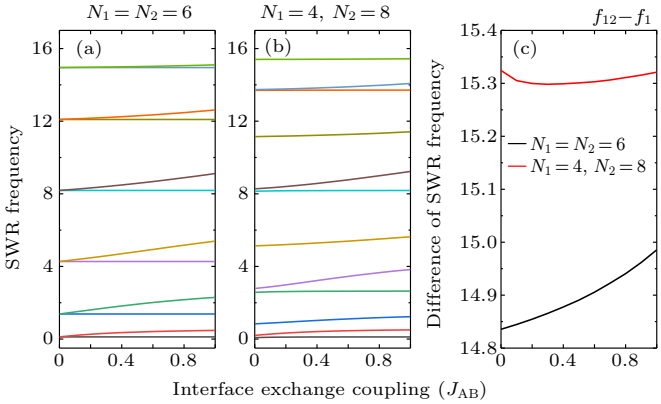



**Fig. 7.** SWR frequency as a function of the interface exchange coupling for symmetric and asymmetric systems with $\alpha = 0.5$. (a) $N_1 = N_2 = 6$, (b) $N_1 = 4$, $N_2 = 8$. (c) Difference of SWR frequency between the energetically highest mode and lowest mode vs. interface exchange coupling for symmetric and asymmetric systems. Other parameters here are the same as those in Fig. 2.

## 4. Conclusion

A higher SWR frequency in bilayer ferromagnetic films is obtained by investigating the dependence of the SWR frequency on the variation of both BQE interaction, interface exchange coupling, symmetry, film thickness, surface anisotropy field, as well as the external magnetic field by means of the linear spin wave approximation and Green's function method. Specifically, the biquadratic to interlayer exchange ratio $\alpha$ leads to a pronounced increase of the SWR frequency, where the variations of the energetically lower two modes are negligible in comparison to other modes. Again, a larger SWR frequency has been achieved in the stronger external magnetic field. As the surface anisotropy field increases from 0 to 1, the SWR frequency displays a clear increase for energetically lower modes, whereas only very small increases are obtained for energetically higher modes. In addition, for the even (odd)

modes, the SWR frequency increases (decreases) as the symmetry of the system is destroyed, whereas the spectrum curves for $m = 6, 8$ ($m = 7, 9$) shift first towards higher (lower) values and then towards the lower (higher) values. Finally, the frequency gap between the energetically highest mode and lowest mode can be increased by increasing the biquadratic to interlayer exchange ratio $\alpha$ and film thickness, and by destroying the symmetry of the system. Our results thus imply that the BQE interaction needs to be taken into consideration to manipulate the SWR frequency and to promote the applications of magnetic material.

## Acknowledgements

Project supported by the Natural Science Foundation of Inner Mongolia of China (Grant No. 2019MS01021), the Research Program of Science and Technology at Universities of Inner Mongolia Autonomous Region, China (Grant No. NJZY21454), and the Theoretical Physics Discipline Development and Communication Platform of Inner Mongolia University (Grant No. 12147216).

## References

[1] Choi S, Lee K S, Guslienko K Y and Kim S K 2007 *Phys. Rev. Lett.* **98** 087205
[2] Ikeda K, Kobayashi K, Ohta K, Kondo R, Suzuki T and Fujimoto M 2003 *IEEE Trans. Magn.* **39** 3057
[3] Kumar M, Kumar A, Singh A, Anshul A, Sharma S and Sati P C 2022 *J. Alloys Compd.* **896** 163074
[4] Kumar A, Sharma P, Qiu F J, Tang J Y and Tan G L 2022 *J. Magn. Magn. Mater.* **564** 170148
[5] Korenivski V 2000 *J. Magn. Magn. Mater.* **215–216** 800
[6] Klemmer T J, Ellis K A, Chen L H, van Dover B and Jin S 2000 *J. Appl. Phys.* **87** 830
[7] Rong J H, Zhang L, Yun G H and Bao L B 2019 *Indian J. Phys.* **93** 207
[8] Zhou J Y, Rong J H, Wang H, Yun G H, Wang Y N and Zhang S F 2022 *Chin. Phys. B* **31** 017601
[9] Wang L, Jing Z X, Liang J, Zhou A R and Li S D 2022 *Chin. Phys. B* **31** 086201
[10] Zhou J Y, Rong J H, Wang H, Zhang S F and Liu L 2022 *Phys. Scr.* **97** 105810
[11] Chai G Z, Yang Y C, Zhu J Y, Lin M, Sui W B, Guo D W, Li X L and Xue D S 2010 *Appl. Phys. Lett.* **96** 012505
[12] Ren Y H, Wu C, Gong Y, Pettiford C and Sun N X 2009 *J. Appl. Phys.* **105** 073910
[13] Zhang C H, Zhang S, Ma T Y, Chai G Z and Wang T 2022 *J. Magn. Magn. Mater.* **561** 169708
[14] Zhong X X, Phuoc N N, Liu Y and Ong C K 2014 *J. Magn. Magn. Mater.* **365** 8
[15] Jiang C J, Fan X L and Xue D S 2015 *Chin. Phys. B* **24** 057504
[16] Ludwig A, Löhndorf M, Tewes M and Quandt E 2001 *IEEE Trans. Magn.* **37** 2690
[17] Zhang F, Miao H L and Lv J Q 2022 *Phys. B* **643** 414053
[18] Snoek J L 1947 *Nature* **160** 90
[19] Bloch F 1930 *Z. Phys.* **61** 206
[20] Holstein T and Primakoff H 1940 *Phys. Rev.* **58** 1098
[21] Rado G T and Weertman J R 1959 *J. Phys. Chem. Solids* **11** 315
[22] Kittel C 1958 *Phys. Rev.* **110** 1295
[23] Seavey M H and Tannenwal P E 1958 *Phys. Rev. Lett.* **1** 168
[24] Qiu R K, Wang Z Y and Zhang Z D 2013 *J. Magn. Magn. Mater.* **331** 92
[25] Qiu R K, Ma F J and Zhang Z D 2015 *J. Magn. Magn. Mater.* **394** 454
[26] Qiu R K and Cai W 2017 *J. Magn. Magn. Mater.* **436** 68
[27] Zhang S H, Rong J H, Wang H, Wang D and Zhang L 2018 *Surf. Sci.* **667** 79
[28] Zhang S H, Rong J H, Wang H, Yun G H, Wang Y N and Bao L B 2018 *J. Magn. Magn. Mater.* **461** 23
[29] Zhang S H, Rong J H, Wang H, Wang D and Zhang L 2018 *J. Supercond. Nov. Magn.* **31** 1499
[30] Ma R J, Rong J H, Zhang S H, Wang H and Yun G H 2020 *J. Phys. Soc. Jpn.* **89** 044705
[31] Ma R J, Zhang S H, Rong J H, Yun G H, Bao L B, Liang Y, Bauer R, Zhen J Y and Chang G S 2021 *Phys. B* **606** 412828
[32] Moriya T 1960 *Phys. Rev.* **120** 91
[33] Yi H, Yu J and Lee S I 2000 *Phys. Rev. B* **61** 428
[34] Rabuffo I, De Cesare L, Caramico D'Auria A and Mercaldo M T 2019 *J. Magn. Magn. Mater.* **472** 40
[35] Wang H, Zhou J Y, Wang Y N and Ma R J 2021 *Indian J. Phys.* **95** 2359
[36] Albayrak E 2020 *Phys. B* **594** 412353
[37] Liu C, Kurokawa Y, Hashimoto N, Tanaka T and Yuasa H 2023 *Sci. Rep.* **13** 3631
[38] Yang J T and Hou J X 2022 *Eur. Phys. J. B* **95** 190
[39] Djerroudi L, Boumeddine F and Tamine M 2019 *Surf. Sci.* **680** 32
[40] Anderson P W 1959 *Phys. Rev.* **115** 2
[41] Kittel C 1960 *Phys. Rev.* **120** 335
[42] Huang N L and Orbach R 1964 *Phys. Rev. Lett.* **12** 275
[43] Glasbrenner J K, Velev J P and Mazin I I 2014 *Phys. Rev. B* **89** 064509
[44] Iwashita T and Uryû N 1976 *Phys. Rev. B* **14** 3090
[45] Iwashita T and Uryû N 1976 *Phys. Lett. A* **58** 113
[46] Zhang X J, Rong J H, Wang H and Wang Y T 2023 *Phys. Scr.* **98** 125952
[47] Grünberg P, Barnas J, Saurenbach F, Fuß J A, Wolf A and Vohl M 1991 *J. Magn. Magn. Mater.* **93** 58
[48] Vohl M, Wolf J A, Grünberg P, Spörl K, Weller D and Zeper B 1991 *J. Magn. Magn. Mater.* **93** 403